Experimental study of wave energy extraction by a dual-buoy heaving system

J. Kim [a], H.J. Koh [b], I.H. Cho [a,*], M.H. Kim [c], H.M. Kweon [d]

[a] *Department of Ocean System Engineering, Jeju National University, Jeju, South Korea*
[b] *Marine & Offshore Engineering Division, Zentech E&C Seoul, South Korea*
[c] *Department of Ocean Engineering, Texas A&M University, College Station, TX, USA*
[d] *Department of Railway Construction and Environmental Engineering, Gyeongju Univeristy, Gyeongbuk, South Korea*

Abstract

The concentric dual-buoy Wave Energy Converter (WEC), which consists of external buoy (hallow-cylinder) with toroidal appendage and cylindrical internal buoy within the moon-pool is suggested in this research and its performance in various wave conditions is studied. The Linear Electric Generator (LEG), consisting of a permanent magnet and coils, is used as a direct Power Take-Off (PTO) system. To maximize the electrical energy extracted from the PTO system, the relative heave motions between the dual buoys must be highly amplified by the multiple resonance phenomena of dual-buoy and internal-fluid motions. The high-performance range can be widened by distributing those natural frequencies with respect to the peak frequency of the wave spectrum. The performance of the newly developed dual-buoy WEC was measured throughout the systematic 1:5.95-model test in regular and irregular waves conducted in a wave tank at Seoul National University. The model-test results are also validated by an independently developed numerical method.

1. Introduction

The global fossil fuel consumption increases each year so it causes serious environmental problems. To solve the problem, many countries have recently adopted policies to reduce the carbon dioxide and enacted renewable energy support. Wave energy, one of the renewable energy resources, is gaining more attention as a sustainable and clean energy and many researches about the appropriate devices for converting wave energy into electrical energy have been carried out (e.g. McCormick, 2007). Wave energy conversion consists of two steps. It first converts wave energy into mechanical energy and then mechanical energy into electrical energy through

generators. Many researchers have proposed numerous devices and evaluated their feasibility by theoretical analysis, scaled model test in laboratory, and prototype test in real sea environment (Drew et al., 2009).

In the real sea environment, the peak frequency of the incident wave spectrum is continuously varying, thus it is very important to design a WEC so that it is efficient for a wide range of incident wave frequencies. Among various types of WEC, point absorber type is designed to induce resonant motion at the peak wave frequency to increase its efficiency (Budal and Falnes, 1975). Bae and Cho (2013) investigated the diffraction and radiation problems of hollow circular cylinders and addressed the characteristics of heaving motion using eigenfunction expansion method. Cho and Kweon (2011) derived the coupled equation of motions with circular buoy and linear electric generator and calculated the generated power which is proportional to the square of heave velocity.

Cho and Kim (2013) and Kim et al. (2014) investigated the characteristics of cylindrical buoy in irregular wave environment and found that the efficiency can be improved if the heave natural frequency of buoy is higher than the peak wave frequency by 15%. Cho and Choi (2014) obtained the heave motion of circular cylinder with linear generator in time domain and investigated the characteristics of power outputs and efficiency. For a power conversion, the linear electric generator consisting of double-sided Halbach array mover and cored slotless stator was used.

There have been other studies dealing with dual buoys with linear generator (e.g. Beatty et al., 2008; Cochet and Yeung, 2012). The Wavebob (Weber et al., 2009), one of point absorber type WECs with dual-buoy system, generated the energy by relative heave motions from the external buoy that moves with waves and resonated internal buoy. The Power buoy (OPT Inc.) is the WEC consisting of the internal buoy with minimal heave motion and the external buoy moving with waves.

If WEC is tuned to resonate, the wave energy can be extracted efficiently due to the amplified motions. However, most existing WECs use the resonance only at single resonant frequency, so it is hard to extract energy outside the narrow resonant frequency region. To overcome this drawback, a newly developed dual-buoy type WEC with three natural frequencies is proposed in this study. This type of WEC can extract wave energy in much broader frequency range when properly designed. Fig. 1 shows the schematic sketch of the dual-buoy WEC. The dual-buoy WEC consists of internal and external buoys centered at the same location. The space between internal and external buoys is filled with fluid. There exist two individual heave natural frequencies from each buoy and one additional natural frequency from the internal fluid pumping motion. The internal fluid presented by the hatched area in Fig. 1 has a number of eigenmodes and the first natural mode is called Piston-mode (or Helmholz mode). If the draft of the internal buoy is relatively smaller than that of the external buoy and its weight is small, then the internal buoy tends to move along with the internal fluid motion. Therefore, the heave resonance characteristics of the internal buoy were not observed in the experiment. So, for the present dual-buoy system, it is important to properly locate the natural frequencies of the external-buoy motion and internal-fluid motion to enhance the overall performance. Moreover, the torus-shaped appendage at the external buoy is intentionally employed to separate the natural frequencies of the internal fluid and external buoy.

The model test in this study utilized the linear electric generator (LEG) consisting of the permanent magnet at the external buoy and coils fixed at the internal buoy as can be seen in Fig. 1. Since the LEG does not require any other extra devices, it is a kind of direct electrical energy generator (e.g. Elwood et al., 2007). It generates electrical energy by relative motions between permanent magnets and coils. Higher relative velocity is very important in designing dual-buoy WEC in that it can generate more energy. The PTO damping, however, may reduce the relative heave motion because it works against it.

In this research, the performance of the dual-buoy system with a wide range of energy extracting frequencies is validated by experiment. Scaled model test ($\lambda = 1/5.95$) was conducted in both regular and irregular wave conditions at Seoul National University. To see the differences in the relative heave motions with and without LEG, the heave displacements were measured with or without 200 Ω resistor which is connected to the coils.

2. Model test

2.1. Experimental model

The proposed dual-buoy system consists of internal and external buoys with same center locations as can be seen in Fig. 1. The air gap between coils and permanent magnet is
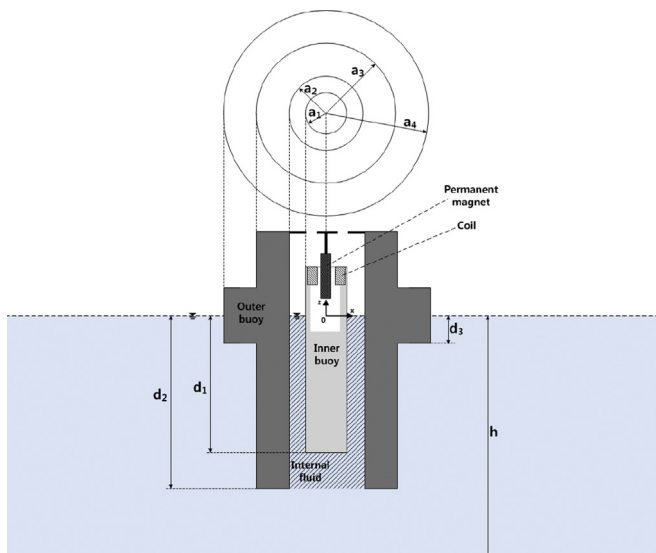

Fig. 1. Definition sketch of a dual-buoy WEC.

Table 1
Specification of a dual-buoy WEC.

Item	Radius [mm]	Draft [mm]	Height [mm]	CoG. (From SW.) [mm]	Mass [kg]	Natural frequency [rad/s]	
						Heave	Pitch
Internal buoy	60 (a_1)	835 (d_1)	1090	−465	9.40	3.24	1.44
External buoy	95 (a_2)	1000 (d_2)	1500	−500	32.6	3.69 (Internal fluid: 3.09)	1.44
	135 (a_3)	168 (d_3)					
	160 (a_4)						

very small, so many possibilities of collisions are expected even with the small relative rotational motion. To avoid the collisions, two vertical shafts are attached at the inner side of the external buoy and two linear bushes are installed at the middle and upper sides of the internal buoy to reduce the friction. Thus, internal buoy moves only through the guide shafts that allows pure heave motion. Due to the friction from the shaft and linear bush, dual-buoy motions are not independent but coupled each other. The buoy system has its own heave natural frequency as well as the natural frequency of the internal fluid. The specifications of a dual-buoy WEC are tabulated in Table 1. The drafts of the internal and external buoys are $d_1 = 835$ mm, $d_2 = 1000$ mm and the masses are $m_1 = 9.4$ kg, $m_2 = 32.6$ kg respectively. The heave natural frequencies of the internal and external buoys can be obtained from Eq. (1) and the piston-mode natural frequency of internal fluid can be calculated by Eq. (2) which is proposed by Fukuda (1977).

$$\omega_{Ni} = \sqrt{\frac{\rho g S_i}{m_i + \mu_i}}, \quad i = 1, 2 \tag{1}$$

$$\omega_{Nf} = \sqrt{\frac{g}{d_2 + 0.41\sqrt{S_f}}} \tag{2}$$

where ρ is water density, g is gravity acceleration, $S_i,(i = 1,2)$ are the water plane areas of the internal and external buoys, $\mu_i,(i = 1,2)$ are the added mass of internal and external buoys. S_f represents the water plane area of the internal fluid. By substituting the values in Table 1 to Eqs. (1) and (2), the natural frequencies of internal buoy ($\omega_{N1} = 3.24$ rad/s), external buoy ($\omega_{N2} = 3.69$ rad/s), and internal fluid ($\omega_{Nf} = 3.09$ rad/s) can be calculated. In addition, the pitch natural frequencies of the buoys are 1.44 rad/s. The pitch natural frequency is designed to have lower natural frequency
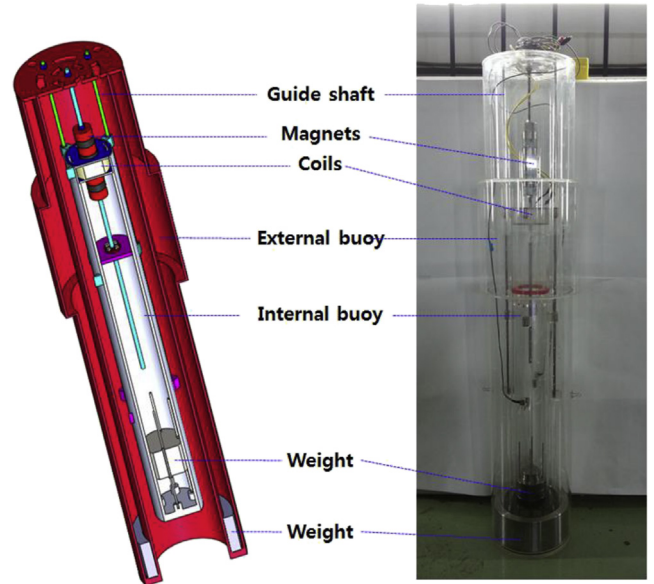

Fig. 3. 3D-drawing (left) and experimental model (right) of the dual-buoy WEC.

than heave natural frequency, so that pitch motion is minimized at the operational frequency range.

Fig. 2 shows the schematic sketch of the linear electric generator, permanent magnet and coil. The permanent magnet consists of four metallic cores inside the five Neodymium magnet. The radius of permanent magnet and core is 22.5 mm and the heights are 30 mm and 20 mm, respectively. The gap between permanent magnet and coil is 7.5 mm and the diameter of coil is 0.65 mm, the number of turns is 1000. The permanent magnet is installed at the guide frame from the external buoy and coil is attached inside the top of the internal buoy (Fig. 1). Fig. 3 shows the 3D-drawing and experimental model of a dual-buoy WECs respectively.
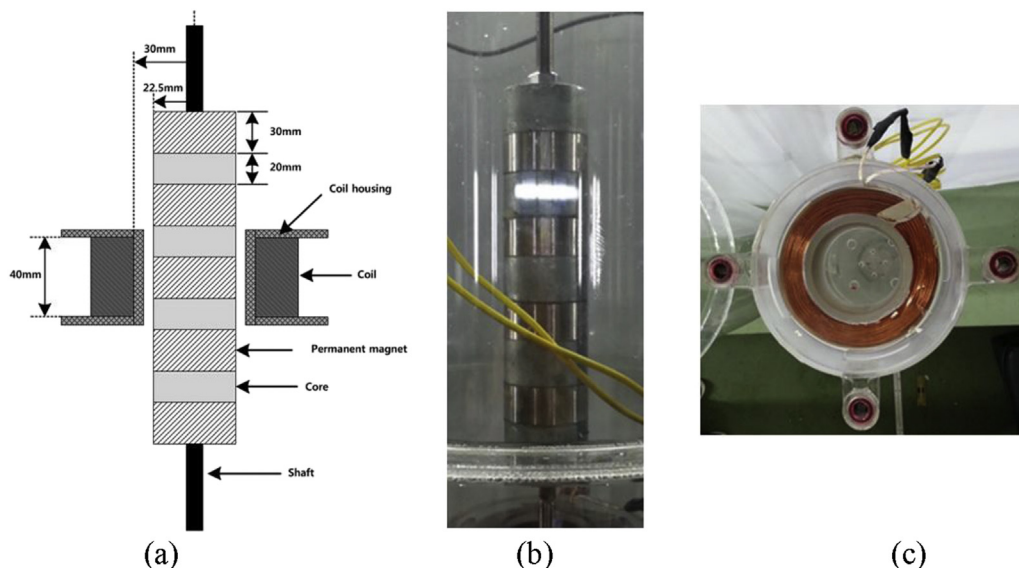

(a)   (b)   (c)

Fig. 2. Modeling of linear electric generator (LEG) (a): Schematic sketch, (b): Permanent magnet, (c): Coil.

2.2. Experimental set-up

The model test was conducted in the towing tank at Seoul National University. The length of the tank is 110 m, width is 8 m, and the water depth is 3.5 m. At the one end of the tank, eight sets of plunger type wave makers which can generate either regular or irregular waves are installed. Wave absorber is installed at the other end to reduce the reflected wave effect. The target model was installed through the hatch of the carriage and placed 30 m away from the wave maker. The capacity type wave gauge was installed at the same distance from the wave maker to measure the incident waves. Since the model size is quite small compared to the tank width, the wall effect is expected to be minimal. Fig. 4 shows the configuration of wave gauge and experimental set up. To measure the heave and pitch motions of dual buoys, three accelerometers (AS-1GB) are attached. In the case of external buoy, two accelerometers are installed at two locations of Fig. 5 and the other one is attached at the top of the internal buoy. As a PTO system, a linear generator was used, as shown in Fig. 2. The voltage and current generated by the linear generator was measured by CompactoRIO NI cRIO-9024 controller and NI-9225, NI-9227 modules. To keep the position of the model against the mean drift force, four lines with soft springs (stiffness = 1.03 N/m) are attached between the vertical rods and the anchor points at the outside wall of the external buoy. Fig. 5 shows the configuration of the mooring and the measurement system. Fig. 6 represents the data acquisition (DAQ) systems, voltmeter and ammeter modules used in this experiment.

During the normal operation of the dual-buoy WEC, the PTO damping ($F_{PTO} = B \cdot I \cdot L$) arises from the linear generator, where B is the strength of a magnetic field, $I (=V/R)$ is current, and L is coil turns. The PTO induced damping further decreases the relative heave motions. The strength of the magnetic field and coil turns are fixed variables determined by the device configuration. In order to generate the current by the linear generator, a resistance (R) should be connected to the coil. Then the measured voltage (V) comes from the relative motions of the two buoys. In the experiment, the generated power was measured by voltage and current using 200 Ω resistor. To investigate the effect of a PTO damping on the buoy dynamics, model test has been conducted with and without PTO system.

In regular wave test, the frequency range was selected as 2.5rad/s $\leq \omega \leq$ 4.2rad/s which includes the natural frequencies of the interior and external buoys and the internal fluid, and total 16 wave frequencies are selected for the regular wave test. Wave steepness was fixed to 0.01. Total 9 cases of irregular wave test were conducted based on the JONSWAP spectrum with various significant wave heights and peak periods combinations. Regular and irregular wave conditions and test cases are summarized in Table 2.

3. Experimental results

3.1. Regular wave test

The experimental results of regular wave tests are expressed as RAOs ($z_{ai}/\zeta_a, (i = 1, 2)$; Response Amplitude Operators) which can be defined by the ratio between incident wave amplitude (ζ_a) and buoy-heave amplitude (z_{ai}). The subscripts $i = 1,2$ represent the internal and external buoys respectively. The effective experimental data was obtained by excluding the reflected wave effect from the wave absorber, and the sampling frequency was 100 Hz. Fig. 7a shows the heave RAOs of the internal and external buoys and the relative heave RAO between them when the resistor was not connected to the linear generator. It is seen that the heave motion of the external buoy is significantly amplified at its resonance frequency ($\omega_{N2} = 3.69$ rad/s) and the heave RAO increases up to 3.3. However, the internal buoy was not amplified near its heave natural frequency ($\omega_{N1} = 3.24$ rad/s), but amplified at the natural frequency of the internal fluid ($\omega_{Nf} = 3.09$ rad/s). This typically happens when the draft of the internal buoy is smaller than that of external buoy. Since the wave exciting forces on the internal buoy are limited due to the surrounded external buoy, the internal buoy motion is mostly dependent on the resonated internal fluid motion. In addition, the friction forces from the guide-shaft at the
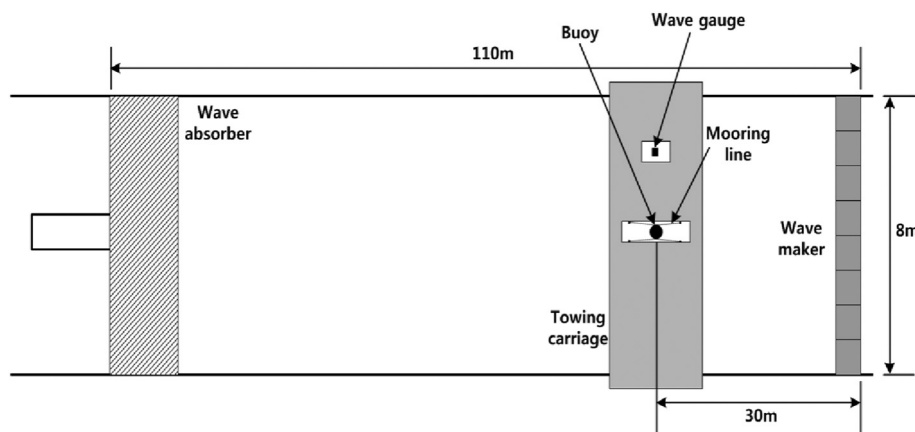

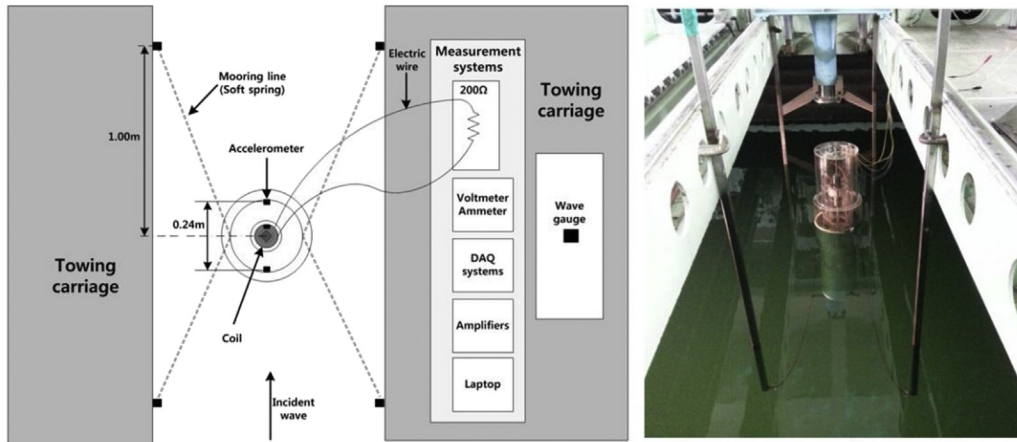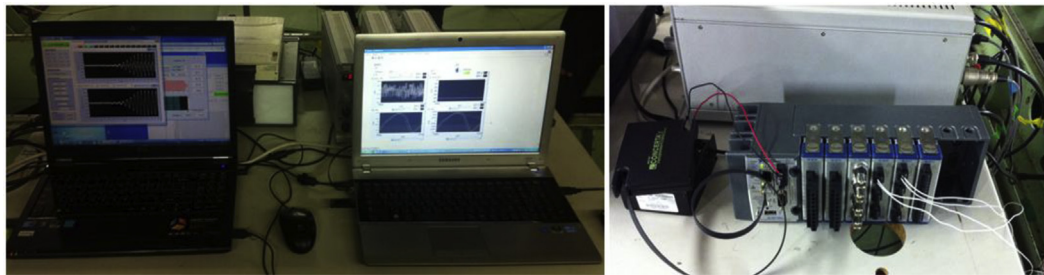Fig. 4. Schematic sketch of the experimental set-up.

Fig. 5. Configuration of mooring and measurement system and photograph of a dual-buoy WEC in wave tank.

(a) DAQ Systems (b) Voltmeter and ammeter modules

Fig. 6. Measurement system for the dual-buoy motion and electric power.

external buoy and the linear bush at the internal buoy induce the coupling effect between dual buoys. So, the internal buoy has a secondary peak at $\omega = 3.5$ rad/s which is close to the resonance frequency of the external buoy, and the external buoy also has a small peak near the resonance frequency of the internal fluid. As a result, in the relative heave motion RAO, two peaks can be observed. Those peaks correspond with two resonance frequencies, i.e. the heave natural

Table 2
Regular and irregular wave conditions.

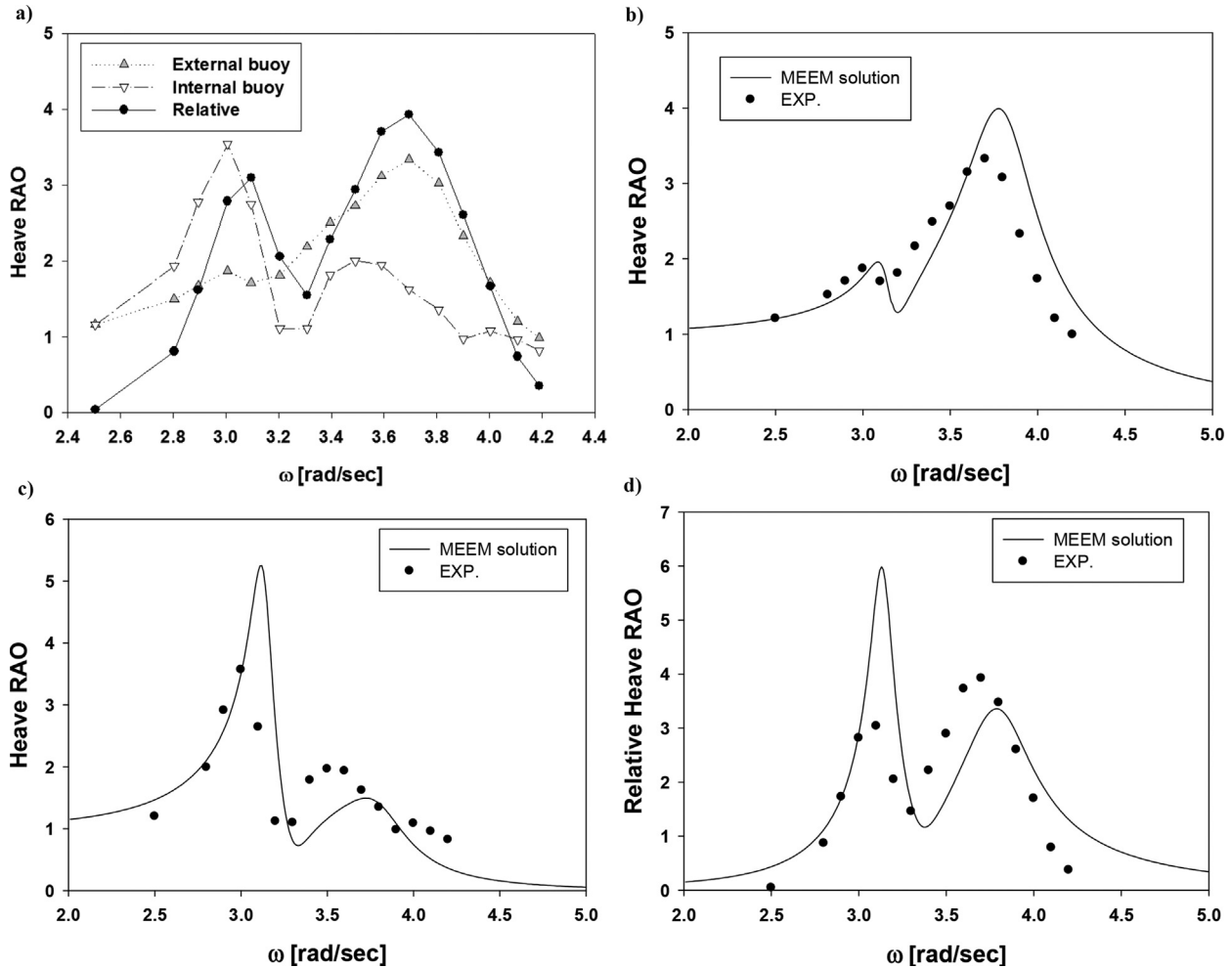|	Regular wave				Irregular wave(JONSWAP spectrum)		
Case	Frequency [rad/s]	Amplitude [m]	Wave steepness	Case	Peak frequency [rad/s]	Significant wave height [m]	Gamma
1	2.5	0.049	0.01	101	2.9	0.074	3.3
2	2.8	0.039	0.01	102	3.0	0.068	3.3
3	2.9	0.037	0.01	103	3.1	0.064	3.3
4	3.0	0.034	0.01	104	3.2	0.060	3.3
5	3.1	0.032	0.01	105	3.3	0.056	3.3
6	3.2	0.030	0.01	106	3.4	0.054	3.3
7	3.3	0.028	0.01	107	3.5	0.050	3.3
8	3.4	0.027	0.01	108	3.6	0.048	3.3
9	3.5	0.025	0.01	109	3.7	0.046	3.3
10	3.6	0.024	0.01				
11	3.7	0.023	0.01				
12	3.8	0.021	0.01				
13	3.9	0.020	0.01				
14	4.0	0.019	0.01				
15	4.1	0.018	0.01				
16	4.2	0.017	0.01				

Fig. 7. a) Experimental results b—c) Comparison of heave RAO of external buoy (b), internal buoy (c), and relative heave RAO (d) between analytic solutions and experimental results in case of disconnecting with LEG.

frequency of the external buoy, and the natural frequency of the internal fluid. This means that the proposed dual-buoy WEC can extract more wave energy from a wide range of incident-wave frequencies compared to a single-resonance system. Fig. 7b—d shows comparisons between experimental and analytical results. The analytical solutions were obtained by using matched eigenfunction expansion method (MEEM). It is based on linear potential theory of the two axisymmetric bodies including diffraction and radiation effects. The potential theory is further improved by adding viscous damping effects which were best estimated from a free-decay test. The comparisons show that the general trend of the experimental and numerical results is very similar and their correlations are very reasonable. Their differences may be attributed to more complex viscous, coupling, and nonlinear effects acting on both internal fluid and buoys.

Fig. 8 shows the heave responses when the 200 Ω resistor of LEG is connected. Compared to Fig. 7a, the resonant heave responses are significantly reduced because of the PTO damping acting in the opposite direction of buoy motion. Particularly, the reduction of the internal buoy motion is greater than that of the external buoy near the resonance frequency.
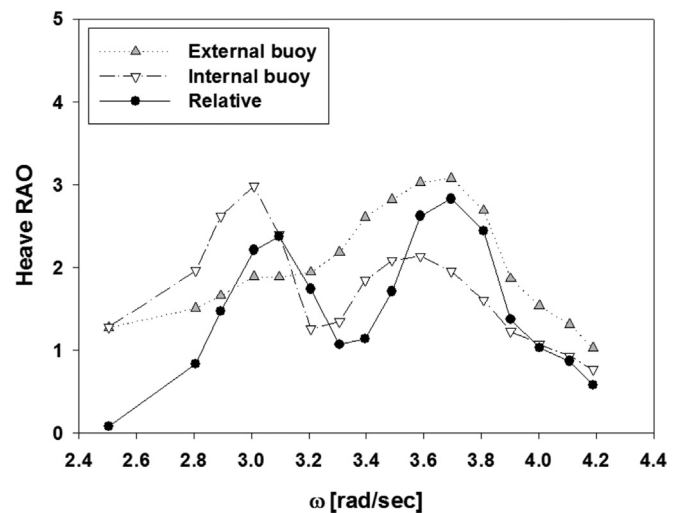

Fig. 8. Heave RAO in case of connecting with LEG.

This is due to the lighter weight of the internal buoy than the external buoy, which is more affected by PTO damping.

One of the most important factors of this dual-buoy WEC system is the relative heave motion which is directly related to
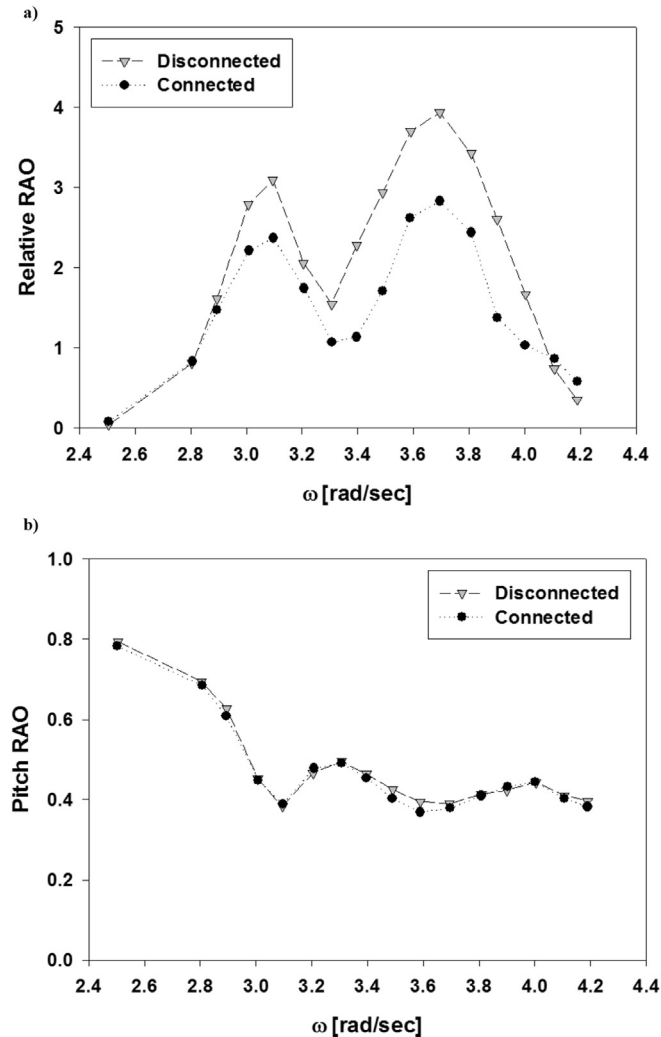
Fig. 9. a) Comparison of relative heave RAO between connecting and disconnecting with LEG. b) Comparison of pitch RAO of a dual-buoy WEC between connecting and disconnecting with LEG.

the electric power generation. Fig. 9a shows the direct comparison of relative heave RAOs with LEG connected and disconnected. Except for the low and high frequency range, the overall relative heave motions are reduced significantly when connected. Fig. 9b shows the pitch motion RAO ($=\theta_a/k\zeta_a$), where θ_a represents the pitch displacement (radian), and k is wave number. As already pointed out, the pitch natural frequency of the WEC is designed to be located at the low frequency range, far away from the incident wave frequencies with prominent energy. So, the pitch motions were not severe during the model test. The PTO damping of LEG affects mostly the heave motion of the buoy, thus the pitch motion responses are little affected by the connection of LEG.

3.2. Irregular wave test

For irregular wave test, JONSWAP wave spectrum with the peakedness factor $\gamma = 3.3$ was used. First, for the verification of the irregular wave test, one set of time series for wave and heave motions is selected and their respective spectra are

calculated. Subsequently, the heave response spectrum is divided by the incident wave spectrum and the square root of the ratio is plotted in Fig. 10a−c and they are compared against the regular-wave-test results. Prior to that, the generated incident wave spectrum was checked against the theoretical input spectrum. Fig. 10a−c shows that there are good correlations between the regular and irregular wave tests, which proves that both experiments were done correctly.

To further analyze the irregular wave test results, the incident wave elevation ($\zeta(t)$), heave motions of the internal and external buoys ($z_1(t)$, $z_2(t)$), and their relative displacements ($z_2(t)-z_1(t)$) are taken and the significant wave amplitude ($\zeta_a)_{1/3}$, significant heave amplitudes of the internal $(z_{1a})_{1/3}$ and external buoys $(z_{2a})_{1/3}$, and the significant relative motion amplitude $(z_{2a} - z_{1a})_{1/3}$ were calculated by zero-crossing method. Figs. 11−13 show the non-dimensionalized significant heave amplitudes of the external and internal buoys and their relative motions. The x-axis shows the peak frequency of the incident wave spectrum. Similar to the regular wave test, the buoy motion is amplified if the peak frequency of the spectrum coincides with the natural frequency, and PTO damping reduces the heave motion amplitude after connection of LEG. From the result of the significant heave amplitude of the external buoy in Fig. 11, the amplitude, near the natural frequency of the external buoy ($\omega_{N2} = 3.69$rad/s), is slightly reduced after connection of LEG, while the reduction in the other frequency range is negligible. On the other hand, the significant heave amplitude of the internal buoy is significantly reduced after connection especially at the natural frequency of the internal fluid $\omega_{Nf} = 3.09$rad/s as can be seen in Fig. 12, but the reduction near the resonant frequency of the external buoy is relatively small. This result again shows that the motion of the external buoy is less affected by the PTO damping than that of the internal buoy.

Fig. 13 shows the significant amplitude of the relative heave motion. The amplification factor remains over 2.5 across the wide range of peak frequency including two resonance frequencies from the internal fluid and the external buoy. This result clearly shows the effectiveness of the energy capture by the present dual-buoy WEC by splitting the resonances from the internal fluid and the external buoy. If buoy is connected to PTO system, the amplified ratio is slightly reduced to 1.91. Since the PTO damping is a function of current, strength of a permanent magnet, and the number of coil turns, it will be a function of resistance after fabrication of a linear generator. For this reason, finding the optimal value of PTO damping and associated resistance value is important to obtain maximum energy. In this experiment, the fixed value of 200 Ω resistor is used. The finding of optimal resistance will be a subject of future study.

The time series of the case 102 (Table 2) which represents the experiment with peak frequency close to the natural frequency of the internal fluid ($\omega_{Nf} = 3.09$ rad/s) is plotted in Figs.14−16. Fig. 14 shows the time series of incident wave elevation and the relative heave motion with disconnected LEG. Fig. 15 shows the same result with connected LEG for power production. As already confirmed from the previous
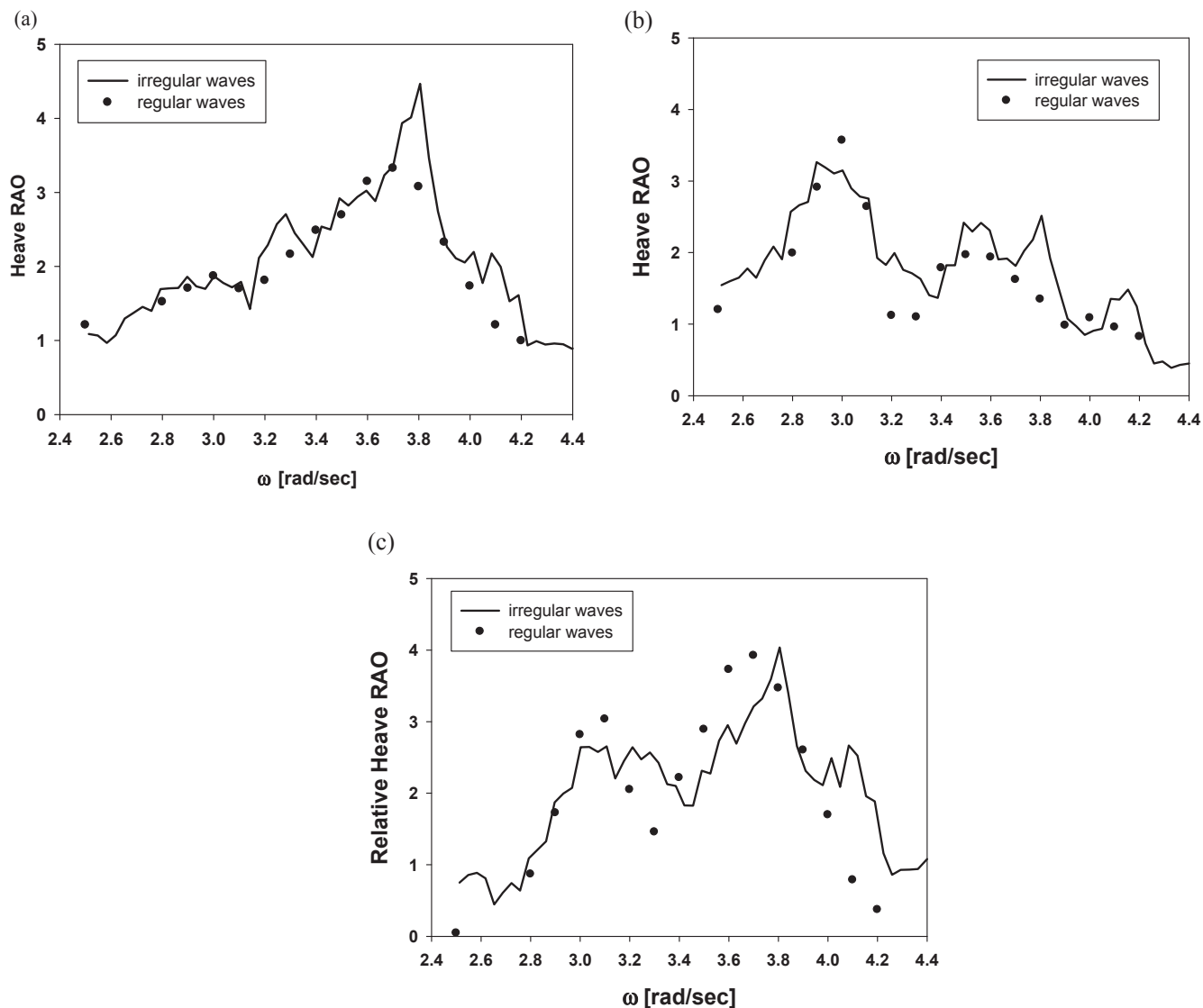
(a)

(b)

(c)

Fig. 10. a—c Comparison of heave RAOs between regular-wave tests and irregular-wave tests in case of disconnecting with LEG.

analysis, relative heave motion in time domain is significantly amplified compared to the incident wave amplitude. In addition, it is also confirmed that the PTO damping reduces the relative heave motion if buoy is connected to the LEG. Finally, the extracted power with the connection of the LEG in the experiment case 102, is plotted in Fig. 16. It is seen that the higher relative heave motion induces more electric power. The maximum power extracted in this experiment is nearly 0.33 W.

4. Conclusions

The proposed dual-buoy WEC in this study utilized dual intrinsic resonance frequencies of the system so that it can extract wave energy from the wide frequency range of incident wave spectrum. The linear electric generator was used as a PTO system to extract electric energy from the incident wave. To examine the performance of the dual-buoy WEC model,

regular and irregular wave tests were conducted in the wave tank at Seoul National University. The energy capture from the linear generator was confirmed by engaging 200 Ω resistor, and its current, voltage, and power were measured. The heave motion responses with LEG connected or disconnected were also checked and compared.

The experimental results show that the external buoy motion is resonated at its own heave natural frequency, as expected. Interestingly, the internal buoy was resonated not at its own heave natural frequency but at the natural frequency of the internal fluid-column pumping motion, which is the typical case when the draft of the internal buoy is relatively smaller than that of the external buoy. The phenomenon can be double checked by the independently developed numerical calculation.

From the regular wave test, the amplified relative heave motion between the internal and external buoys was observed at the natural frequencies of the external buoy and the internal
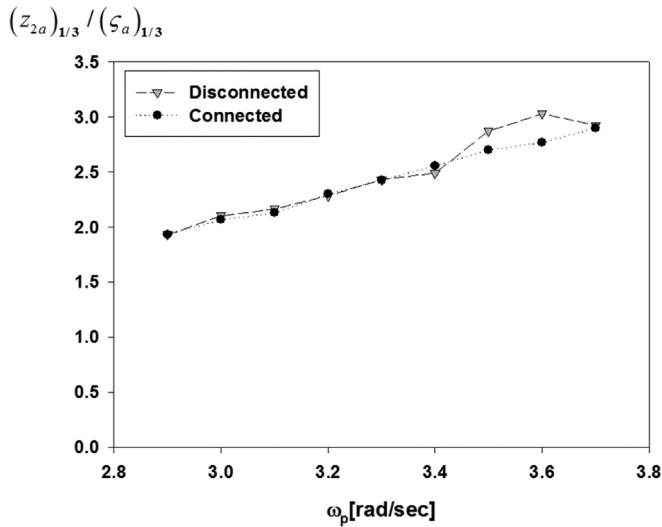
$(z_{2a})_{1/3} / (\varsigma_a)_{1/3}$

Fig. 11. Comparison of the significant heave motion amplitude of external buoy between connecting and disconnecting with LEG.
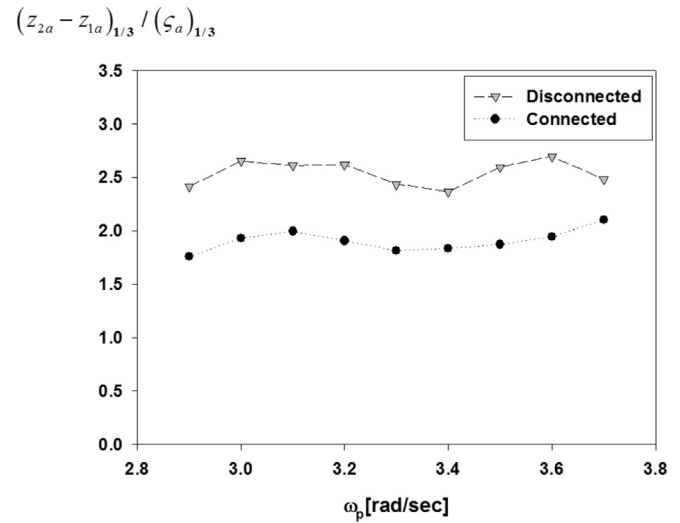
$(z_{1a})_{1/3} / (\varsigma_a)_{1/3}$

Fig. 12. Comparison of the significant heave motion amplitude of internal buoy between connecting and disconnecting with LEG.

$(z_{2a} - z_{1a})_{1/3} / (\varsigma_a)_{1/3}$

Fig. 13. Comparison of the significant relative heave motion amplitude of two buoys between connecting and disconnecting with LEG.

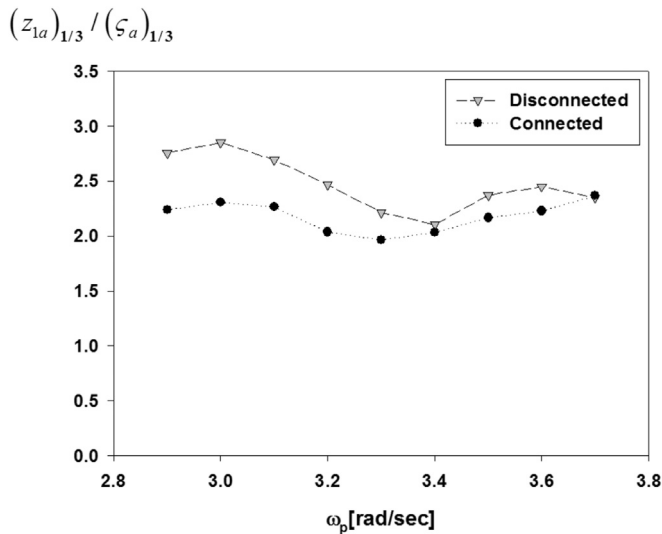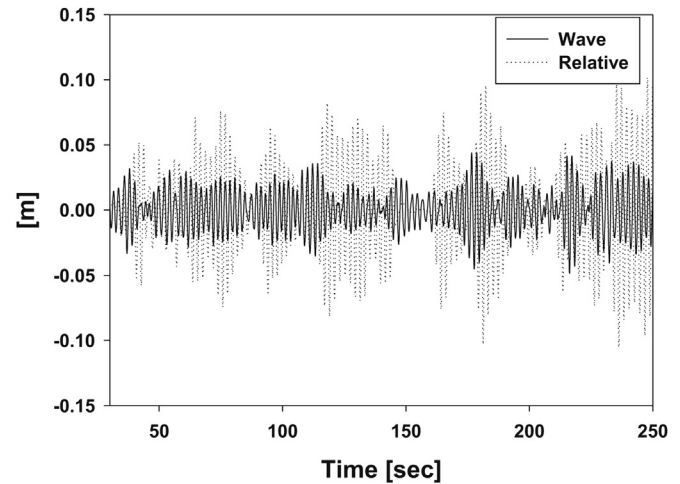Fig. 14. Time series of incident wave and relative heave motion (case 102) in case of disconnecting with LEG.
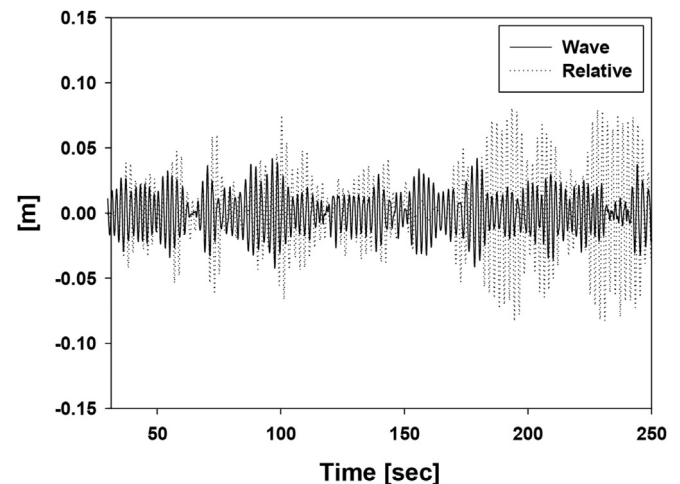
Fig. 15. Time series of incident wave and relative heave motion (case 102) when connecting with LEG.

fluid. By having dual peaks, the appreciable energy capture can be done at a wide range of incident wave frequency. After connecting a 200 Ω resistor to LEG, the heave motions were appreciably reduced especially near the resonance frequencies due to the PTO damping, and the reduction rate of the internal buoy was greater than that of the external buoy because of its light weight.

The irregular wave test actually shows that the energy capture can be done from a wide range of incident wave frequencies. In the wide range, the significant relative motion amplification factor compared to significant incident wave amplitude is about 2 with PTO system acting. This result confirmed that the dual-buy WEC can be efficiently operated for a variety of wave conditions. The irregular wave test results were double checked against the regular wave test results by using the relevant spectral analysis and their correlations were very reasonable.
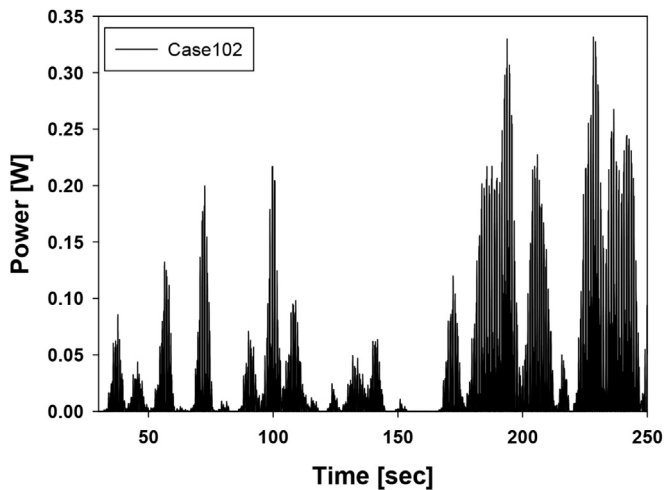
Fig. 16. Time series of extracted power (case 102) in case of connecting with LEG.

The time series of the irregular wave test indicated that the higher power was generated at the time of the higher relative heave motion. The maximum power extracted from the model test was about 0.33 W. The extracted power was relatively weak because the connected resistance capacity was fixed at 200 Ω for convenience. If the optimal value of the resistance is used, much higher power can be produced, which is the subject of forthcoming study.

Acknowledgment

References

Bae, Y.H., Cho, I.H., 2013. Characteristics of heaving motion of hollow circular cylinder. J. Ocean Eng. Technol. 27 (5), 43−50.

Beatty, S.J., Buckham, B.J., Wild, P., 2008. Frequency response tuning for a two body heaving wave energy converter, Proc. 18th Intl. Conf. Offshore and Polar Eng. (ISOPE), Vancouver.

Budal, K., Falnes, J., 1975. A resonant point absorber of ocean wave power. Nature 256, 478−479.

Cho, I.H., Kweon, H.M., 2011. Extraction of wave energy using the coupled heaving motion of a circular cylinder and linear electric generator. J. Ocean Eng. Technol. 25 (6), 9−16.

Cho, I.H., Kim, M.H., 2013. Enhancement of wave-energy-conversion efficiency of a single power buoy with inner dynamic system by intentional mismatching strategy. Ocean Syst. Eng. Int. J. 3 (3).

Cho, I.H., Choi, J.Y., 2014. Design of wave energy extractor with a linear electric generator, part II. Linear generator. J. Korean Soc. Mar. Environ. Energy 17 (3), 174−181.

Cochet, C., Yeung, R.W., 2012. Two-component axisymmetric wave-energy absorber − analysis of dynamics and geometric proportions. In: The 27th International Workshop on Water Waves and Floating Bodies, Copenhagen, Denmark.

Drew, B., Plummer, A.R., Sahinkaya, N.N., 2009. A review of wave energy converter technology. Proc. Inst. Mech. Eng. Part A J. Power Energy 233, 887−902.

Elwood, D., Rhinefrank, K., Prudell, J., Schacher, A., Hogan, P., Vander Meulen, A., von Jouanne, A., Brekken, T., Yokochi, A., Yim, S.C., 2007. Experimental and numerical modeling of direct-drive wave energy extraction devices, Offshore Mechanics and Arctic Engineering Conference, San Diego, CA, Paper No.OMAE2007-29728.

Fukuda, K., 1977. Behavior of water in vertical well with bottom opening of ship and its effects on ship-motion. J. Soc. Nav. Archit. Jpn. 141, 107−122.

Kim, J.R., Bae, Y.H., Cho, I.H., 2014. Design of wave energy extractor with a linear electric generator, part I. Design of wave power buoy. J. Korean Soc. Mar. Environ. Energy 17 (2), 146−152.

McCormick, M.E., 2007. Ocean Wave Energy Conversion. Dover Publication.

Weber, J., Mouwen, F., Parrish, A., Robertson, D., 2009. Wavebob-research and development network and tools in the context of systems engineering. Proceedings of 8th European Wave Tidal Energy Conference, 416−410.